VPS VIBRATIONS IN PHYSICAL SYSTEMS

DOI: 10.21008/j.0860-6897.2022.2.05
Vibrations in Physical Systems, 2022, 33(2), 2022205

Analysis of Sound Absorption Performance of Acoustic Absorbers Made of Fibrous Materials

Mirosław MEISSNER, Tomasz G. ZIELIŃSKI

Institute of Fundamental Technological Research, Polish Academy of Sciences, Pawińskiego 5B, 02-106 Warsaw

Corresponding author: Mirosław MEISSNER, email: mmeissn@ippt.pan.pl

Abstract Absorbing properties of multi-layer acoustic absorbers were modeled using the impedance translation theorem and the Garai and Pompoli empirical model, which enables a determination of the characteristic impedance and propagation constant of fibrous sound-absorbing materials. The theoretical model was applied to the computational study of performance of single-layer acoustic absorber backed by a hard wall and the absorber consisting of one layer of absorbing material and an air gap between the rear of the material and a hard back wall. Simulation results have shown that a high thickness of absorbing material may cause wavy changes in the frequency relationship of the normal and random incidence absorption coefficients. It was also found that this effect is particularly noticeable for acoustic absorbers with a large thickness of air gap between the absorbing material and a hard back wall.

Keywords: sound absorption, multi-layer absorber, surface impedance, fibrous materials, air gap.

1. Introduction

A technique commonly employed for improving the acoustics of hard-walled rooms consists in increasing a sound absorption on room walls [1]. This goal can be achieved by using acoustic absorbers or different configurations of sound absorbing materials for acoustic treatment of the room [2]. In this context, the acoustic treatment aimed at improving a low-frequency spectral flatness in the room frequency response is particularly important [3]. In the wave-based models utilized to predict the acoustic field in rooms, absorbing properties of room walls are characterized by the wall impedance at normal incidence of sound. This impedance can be determined by either directly using impedance measurements [4] or indirectly using empirical models. In this paper the Garai and Pompoli empirical model [5] and the impedance translation theorem [6] are applied to determine the impedance at the front surface of multi-layer acoustic absorbers made of fibrous materials. The paper is arranged as follows. Section 2 presents a theory applied to model the multi-layer absorbers, shows the details of the Garai and Pompoli empirical model, and then provides formulas for the impedance of a single layer absorber backed by the hard wall and the absorber consisting of single layer of absorbing material and an air gap between the material and the back hard wall. Section 3 specifies values of the input parameters adopted in the computer simulation, and then presents the calculation results obtained for various structures of acoustic absorbers, taking into account different absorption properties of the fibrous material and different thickness of the layer. Finally, the original findings of this study and concluding remarks are given in Sect. 4.

2. Theoretical model

The relationship between reverberation and sound damping in enclosures is a fundamental issue in room acoustics because reverberation plays an important role in every aspect of room acoustics and is the main criterion for assessing the acoustic quality of enclosures. Due to the small dimensions of typical rooms, the absorption of sound in the air can be neglected. Thus, the sound damping inside rooms is only provided by absorbing room walls. These walls are assumed to be locally reacting, therefore, the sound pressure p satisfies the following boundary condition on wall surfaces

$$\frac{\partial p}{\partial n} = -\varrho_0 \frac{\partial u_n}{\partial t} = -\frac{\varrho_0}{Z}\frac{\partial p}{\partial t}, \tag{1}$$

where $\partial/\partial n$ denotes a derivative in a direction outward normal to the wall, ρ_0 is the air density, $u_n = p/Z$ is the normal velocity component and Z is the wall impedance. Lightly damped rooms represent the simplest case of enclosures with absorbing walls. In theoretical models, damping properties of these walls are

characterized by the real-valued wall impedance Z_c satisfying the condition $z_c = Z_c/Z_0 \gg 1$, where $Z_0 = \rho_0 c_0$ is the characteristic impedance of air and c_0 is the sound speed in air. Although the condition of the constant value of wall impedance is commonly used in room acoustic simulations, it is more appropriate to consider in the theoretical model that the impedance of hard walls, such as concrete or brick walls, is frequency dependent. The impedance of the real hard walls can be determined based on values of the random incidence absorption coefficient α found in the literature. As shown in Tab. 1, this coefficient is known in certain octave bands, thus using the following formula [7]

$$\alpha = \frac{8}{z_c}\left[1 - \frac{2}{z_c}\ln(1+z_c) + \frac{1}{1+z_c}\right] \tag{2}$$

and the values of α from Tab. 1, the impedance z_c for these octave bands is computed. To predict the frequency dependence of z_c from this calculation data, a logarithmic regression was used and the result is

$$z_c = A + B\ln\left(\frac{f}{f_{\text{ref}}}\right), \tag{3}$$

where $A = 755.3$ and $B = -73.7$ are non-dimensional coefficients, f is the sound frequency in Hz and $f_{\text{ref}} = 1$ Hz. The graph illustrating the frequency dependence of z_c in the frequency range 80–6000 Hz is depicted in Fig. 1. As can be seen from this figure, with increasing frequency, a rapid decrease in the impedance z_c occurs at low frequencies, and at higher frequencies, the observed decrease in this impedance becomes smaller and smaller. Equation (3) was used to calculate the absorption coefficient α for octave bands with a centre frequency from 125 Hz to 4000 Hz (Tab. 1), and the comparison of experimental and computed results confirms correctness of this equation in predicting changes in the impedance z_c with frequency.

Table 1. Random incidence absorption coefficient for hard surfaces.

Hard surfaces (brick walls, plaster, hard floors, etc.)	Centre frequency of octave band (Hz)					
	125	250	500	1000	2000	4000
Experimental data from Ref. [7]	0.02	0.02	0.03	0.03	0.04	0.05
Predictions from Eq. (3)	0.0196	0.0225	0.0263	0.0317	0.0398	0.0538

The poor acoustic quality of rooms with hard walls is due to a number of acoustic flaws such as long reverberation time and unwanted sound coloration, which may prevent the correct sound perception in rooms where speech, music or listening is part of normal use. Acoustics of hard-walled rooms can be improved by placing acoustic absorbers made of fibrous or porous materials on room walls. However, in many cases, the use of these materials on a floor is impossible for practical reasons, therefore the acoustic treatment of rooms most often relies on installing acoustic absorbers on a ceiling and/or lateral walls.

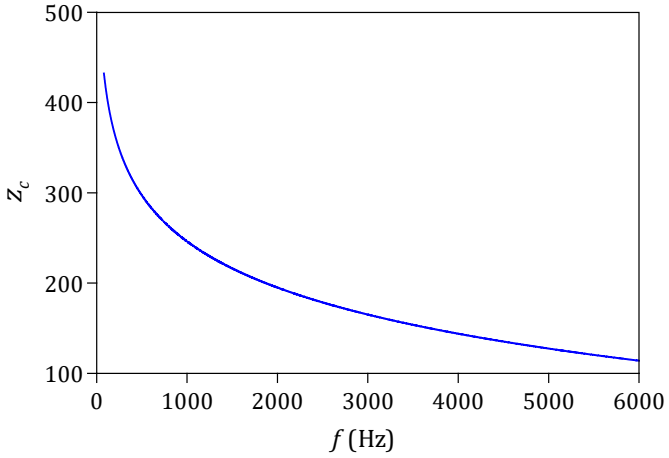

Figure 1. Frequency dependence of normalized impedance z_c calculated for hard walls using Eq. (3).

In order to achieve higher sound absorption performance at different frequency bands, the acoustic absorbers used in practice are often multi-layered. The structure of such an absorber is shown in Fig. 2.

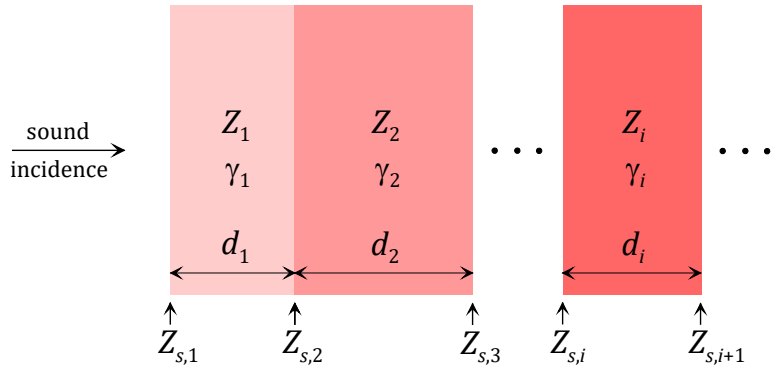

Figure 2. Diagram of multi-layer acoustic absorber.

In this figure $Z_{s,i}$ and $Z_{s,i+1}$ are the surface impedances of the layers i and $i+1$, and Z_i, γ_i, d_i represent the complex characteristic impedance, the complex characteristic propagation constant and the thickness of layer i. If the quantities $Z_{s,i+1}$, Z_i, γ_i, d_i are known, the impedance $Z_{s,i}$ can be determined from equation

$$Z_{s,i} = \frac{Z_i\left[Z_i - \mathrm{j}Z_{s,i+1}\cot(\gamma_i d_i)\right]}{Z_{s,i+1} - \mathrm{j}Z_i\cot(\gamma_i d_i)}, \tag{4}$$

where $\mathrm{j} = \sqrt{-1}$. This equation is commonly referred to as the impedance translation theorem [6]. It follows from Eq. (4) that this theorem relates a surface impedance at one side of a layer to that at the other. In this manner, one may apply this theorem as many times as necessary to compute a surface impedance at any interface in a layered acoustic absorber. The characteristic impedance Z_i of the material and the characteristic propagation constant γ_i can be determined experimentally using the acoustic standing wave method. On the other hand, these parameters can be determined theoretically by means of empirically based models such as the model for fibrous materials by Delany and Bazley [8]. The power-law relations proposed in the work [8] were used by Garai and Pompoli in their empirical model for absorbing materials made of polyester fibres [5]. This model was experimentally verified on a set of 38 samples of fibrous materials with different density and thickness values. This model specifies the impedance Z_i and the propagation constant γ_i as a function of the sound frequency f and the airflow resistivity σ_i of the absorbing material according to the formulas

$$Z_i = Z_0\left[1 + 0.078\left(\frac{\rho_0 f}{\sigma_i}\right)^{-0.623} - \mathrm{j}0.074\left(\frac{\rho_0 f}{\sigma_i}\right)^{-0.66}\right], \tag{5}$$

$$\gamma_i = k_0\left[1 + 0.121\left(\frac{\rho_0 f}{\sigma_i}\right)^{-0.53} - \mathrm{j}0.159\left(\frac{\rho_0 f}{\sigma_i}\right)^{-0.571}\right], \tag{6}$$

where $k_0 = 2\pi f/c_0$. As with other empirically based models, this model has limited validity. Garai and Pompoli do not provide information regarding the range of validity of their formulas, but examination of the sample data, that they provide, indicate that Eqs. (5) and (6) were developed for the range

$$0.02 < \rho_0 f/\sigma_i < 8.4. \tag{7}$$

The absorption performance of multi-layer acoustic absorbers is assessed on the basis of the values of two quantities: the normal incidence absorption coefficient α_n and the random incidence absorption coefficient α. When $Z_{s,1}$ is known, these coefficients can be calculated using the following formulas [7]

$$\alpha_n = 1 - \left|\frac{Z_{s,1} - Z_0}{Z_{s,1} + Z_0}\right|^2 = \frac{4\zeta_r}{|\zeta|^2 + 2\zeta_r + 1}, \tag{8}$$

$$\alpha = \frac{8\zeta_r}{|\zeta|^2}\left[1 - \frac{\zeta_r}{|\zeta|^2}\ln(1 + 2\zeta_r + |\zeta|^2) + \frac{\zeta_r^2 - \zeta_i^2}{\zeta_i|\zeta|^2}\arctan\left(\frac{\zeta_i}{1 + \zeta_r}\right)\right], \tag{9}$$

where $\zeta_r = \mathrm{Re}\left(Z_{s,1}/Z_0\right)$ and $\zeta_i = \mathrm{Im}\left(Z_{s,1}/Z_0\right)$ are real and imaginary parts of the surface impedance $Z_{s,1}$ normalized by the characteristic impedance of air and $|\zeta|^2 = \zeta_r^2 + \zeta_i^2$. Since $Z_{s,1}$ is frequency dependent, so the absorption coefficients α_n and α also change with the sound frequency.

The simplest application of the impedance translation theorem (4) allows to determine the surface impedance $Z_{s,1}$ of a single layer of absorbing material with the thickness of d_1 backed by a perfectly rigid wall. In this case, the impedance $Z_{s,2}$ goes to infinity and Eq. (4) simplifies to

$$Z_{s,1} = -\mathrm{j}Z_1 \cot(\gamma_1 d_1). \tag{10}$$

When this material is backed by a wall with the surface impedance Z_c, Eq. (4) leads to the expression

$$Z_{s,1} = \frac{Z_1[Z_1 - \mathrm{j}Z_c \cot(\gamma_1 d_1)]}{Z_c - \mathrm{j}Z_1 \cot(\gamma_1 d_1)}. \tag{11}$$

Among the absorbers often used in practice are also systems consisting of single layer of absorbing material and air gap with the thickness of d_2 between the rear of the material and the back wall. This configuration is typical for suspended ceilings. In this case the formula for the impedance $Z_{s,1}$ is as follows

$$Z_{s,1} = \frac{Z_1\left[Z_1 - \mathrm{j}Z_{s,2} \cot(\gamma_1 d_1)\right]}{Z_{s,2} - \mathrm{j}Z_1 \cot(\gamma_1 d_1)}, \tag{12}$$

where the surface impedance of the air gap $Z_{s,2}$ is given by

$$Z_{s,2} = -\mathrm{j}Z_0 \cot(k_0 d_2), \tag{13}$$

when the wall backing the gap is perfectly rigid, or is expressed as

$$Z_{s,2} = \frac{Z_0[Z_0 - \mathrm{j}Z_c \cot(k_0 d_2)]}{Z_c - \mathrm{j}Z_0 \cot(k_0 d_2)}, \tag{14}$$

when the back wall is not perfectly rigid and has a finite surface impedance Z_c.

3. Analysis of computer simulation results

The performance of acoustic absorbers has been numerically tested for the most commonly used sound-absorbing systems: a single-layer acoustic absorber backed by a hard wall and the absorber consisting of one layer of absorbing material and an air gap between the rear of the material and a hard back wall. The values of input parameters adopted in the computer simulation are listed in Tab. 2. In the simulation, the value of the airflow resistivity σ_1 was limited to 5000 Pa·s/m^2, because according to the condition (7), this quantity should not exceed the value $\rho_0 f_{\min}/0.02 = 5143$ Pa·s/m^2. The impedance at the front of the absorbers was determined from Eqs. (11), (12) and (14), and the material characteristic impedance and propagation constant present in these formulas were computed using Eqs. (5) and (6). The effectiveness of sound attenuation by acoustic absorbers was assessed on the basis of the values of the normal and random incidence absorption coefficients α_n and α, calculated from Eqs. (8) and (9).

Table 2. Values of input parameters adopted in computer simulation.

Quantity	Symbol	Unit	Value
Air density	ρ_0	kg/m^3	1.21
Sound speed in air	c_0	m/s	343
Sound frequency	f	Hz	85–6000
Airflow resistivity of fibrous material	σ_1	Pa·s/m^2	1000–5000
Thickness of fibrous material	d_1	cm	3–15
Thickness of air gap	d_2	cm	15

The frequency dependences of α_n for a single-layer absorber with a fibrous material of the thickness of 4 cm, for different values of the airflow resistivity σ_1 are shown in Fig. 3a. As expected, an increase in the value of σ_1 results in a significant improvement in sound absorption over the entire frequency range. However, an unfavorable phenomenon is a decrease in the absorber efficiency in the frequency range 3000 ÷ 5000 Hz. More complex changes in the coefficient α_n are seen when the airflow resistivity σ_1 is constant, but the thickness d_1 of the absorbing material varies since the frequency dependence of α_n becomes more and more wavy as d_1 increases (Fig. 3b). To investigate this effect in more detail, in Fig. 4a the frequency dependence of the random incidence absorption coefficient α for the absorber with the layer thickness d_1 of 15 cm and the airflow resistivity σ_1 of 1000 Pa·s/m^2 is shown. This figure indicates that in this case there are more regular wavy changes in the relationship between α and the frequency *f*.

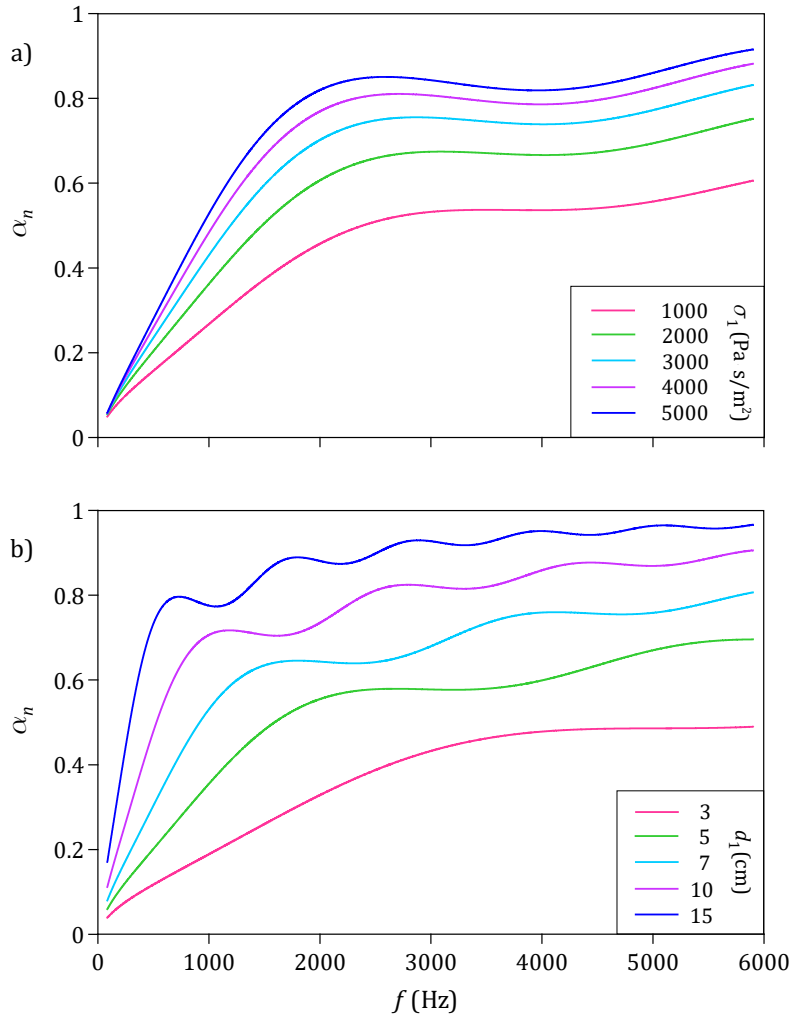

Figure 3. Frequency dependence of normal incidence absorption coefficient α_n for different configurations of single-layer absorber with hard back wall: a) layer thickness d_1 = 4 cm, airflow resistivity σ_1 from range 1000 ÷ 5000 Pa·s/m², b) layer thickness d_1 from range 3 ÷ 15 cm, airflow resistivity σ_1 = 1000 Pa·s/m².

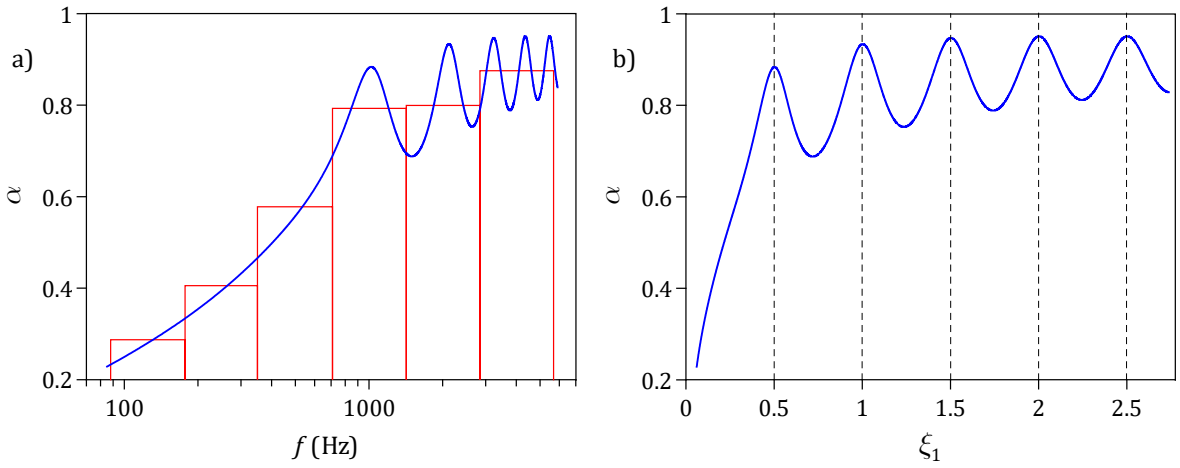

Figure 4. a) Frequency dependence of random incidence absorption coefficient α for single-layer absorber with hard back wall having layer thickness d_1 = 15 cm and airflow resistivity σ_1 = 1000 Pa·s/m², horizontal red lines indicate computed values of α in octave bands 125 ÷ 4000 Hz, b) dependence of α on parameter ξ_1 for this absorber.

If changes in α are defined as a function of the parameter $\xi_1 = d_1/\lambda_1$, where $\lambda_1 = 2\pi/Re(\gamma_1)$ is the acoustic wavelength in the material, then an interesting regularity is noted, namely, the maxima in this relationship fall exactly for the parameter ξ_1 equal to $n/2$, where $n = 1{,}2 \ldots 5$ (Fig. 4b). This proves that absorption peaks appear at the frequencies that correspond to the half-wavelength resonance in the material layer. The simulation has shown that this regularity is the result of unusual changes in the real and imaginary parts of impedance $Z_{s,1}$ with the frequency. It turns out that if these changes are determined in the function of the parameter ξ_1, then the real part of this impedance reaches local maxima when $\xi_1 = n/2$ (Fig. 5a). It is also worth adding that the imaginary part of this impedance is zero not only for ξ_1 equal to $n/2$, but also when ξ_1 is equal to $(2n-1)/4$ (Fig. 5b).

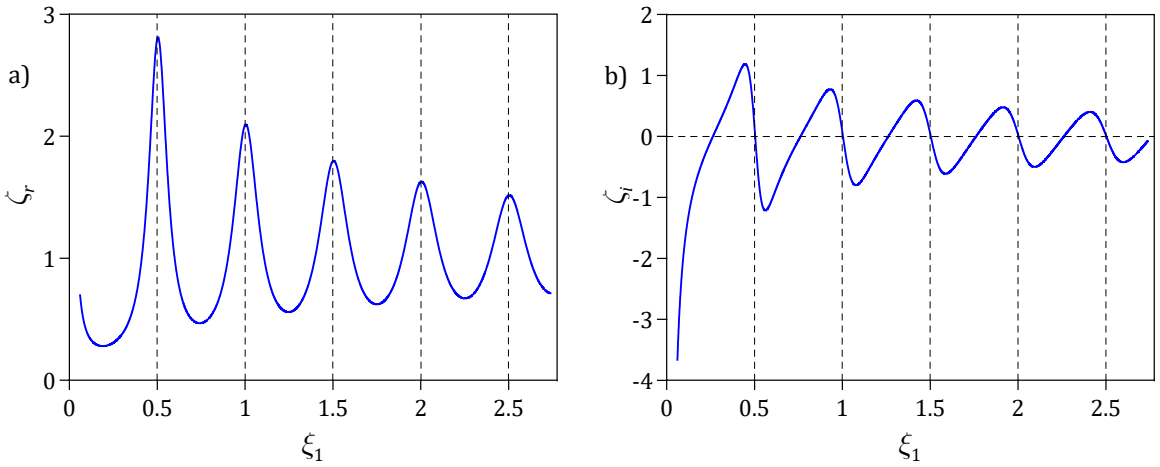

Figure 5. Changes in real (a) and imaginary (b) parts of impedance $Z_{s,1}$ with parameter ξ_1 for absorber with layer thickness d_1 = 15 cm and airflow resistivity σ_1 = 1000 Pa·s/m^2.

In the next part of the computer simulation, the performance of acoustic absorbers with an air gap was investigated. The thickness of the layer and its absorbing properties are the same as for a single-layer absorber, but the main difference between these absorbers is that there is the air gap with the thickness d_2 of 15 cm between the material and the hard back wall. In order to compare simulation results with those obtained for a single-layer absorber, the calculation data shown in Figs. 6–8 correspond to those presented in Figs. 3–5 in terms of substantive content. Figure 6a shows the frequency dependences of α_n for the absorbing material with the layer thickness d_1 of 4 cm and different values of the airflow resistivity σ_1. As may be seen, the introduction of an air gap results in an improvement of absorber performance at low frequencies. However, it is accompanied by a decrease in the sound absorption in some frequency ranges due to the formation of dips in the frequency dependence of α_n. The depth of these dips increases with growing the airflow resistivity (Fig. 6a). On the other hand, as shown in Fig. 6b, the number of these dips increases with increasing the thickness d_1 of absorbing material.

In Figure 7a, the frequency dependence of the random incidence absorption coefficient α for the absorber with the layer thickness d_1 of 15 cm and the airflow resistivity σ_1 of 1000 Pa·s/m^2 is depicted. Comparison of these results with the results presented in Fig. 4a shows that the air gap causes a significant increase in wavy changes in the relationship between α and the frequency. This effect can be explained if the changes of the coefficient α are determined as a function of the parameter ξ_2 defined as

$$\xi_2 = \frac{(d_1 + d_2)f}{c_{\text{av}}}, \tag{15}$$

where $c_{\text{av}} = (d_1 + d_2)/(d_1/c_1 + d_2/c_0)$ is the average phase velocity in the absorber and $c_1 = \lambda_1 f$ is the phase velocity in the material, because, as shown in Fig. 7b and Fig. 8a, the coefficient α and the real part of the impedance $Z_{s,1}$ reach local maxima for the parameter ξ_2 equal to $n/2$, where n represents natural numbers from 1 to 10. Therefore, the condition for the maximal absorption can be written as

$$\frac{(d_1 + d_2)f}{c_{\text{av}}} = \frac{d_1}{\lambda_1} + \frac{d_2}{\lambda_0} = \frac{n}{2}, \tag{16}$$

where $\lambda_0 = c_0/f$ and the quantity c_{av}/f can be interpreted as the average wavelength in the absorber. This means that absorption peaks in the frequency dependence of the absorption coefficient α appear as a result of the half-wavelength resonance between the front of the absorber and the hard back wall.

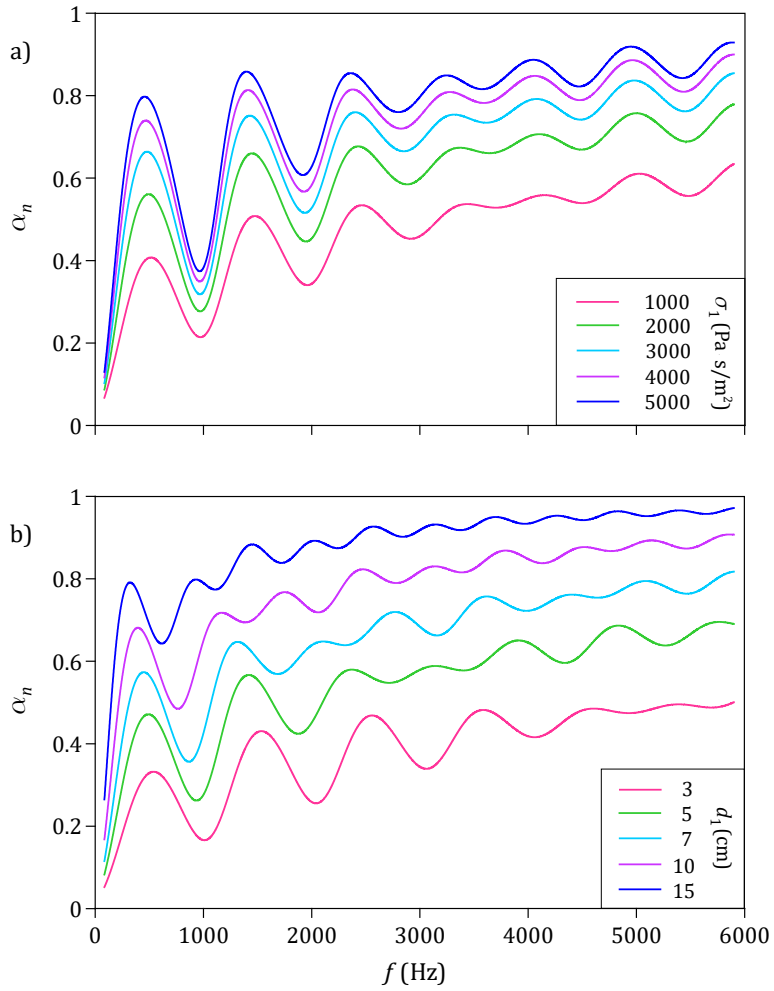

Figure 6. Frequency dependence of normal incidence absorption coefficient α_n for different configurations of absorber with single layer of absorbing material and air gap with thickness d_2 = 15 cm between material and hard back wall: a) layer thickness d_1 = 4 cm, airflow resistivity σ_1 from range 1000 ÷ 5000 Pa·s/m², b) layer thickness d_1 from range 3 ÷ 15 cm, airflow resistivity σ_1 = 1000 Pa·s/m².

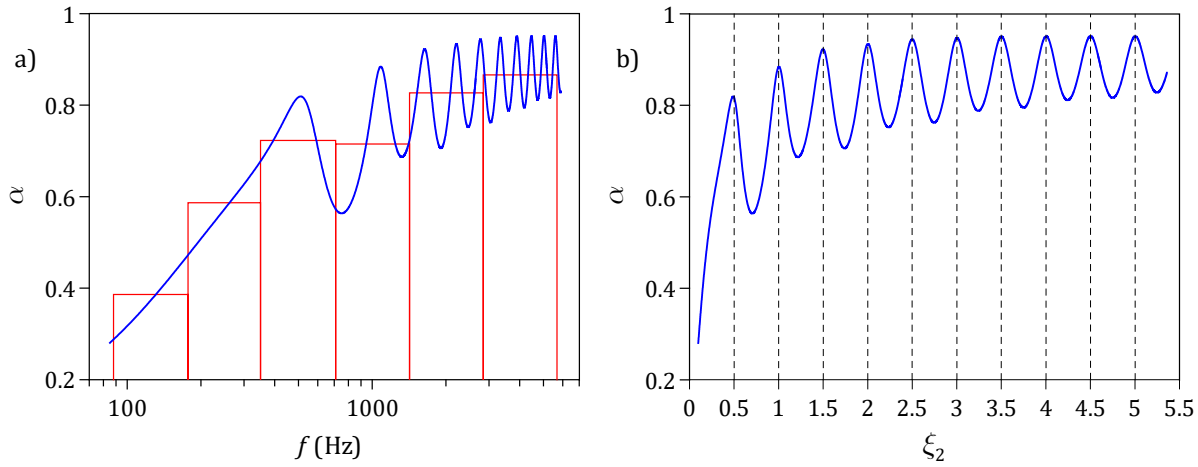

Figure 7. a) Frequency dependence of random incidence absorption coefficient α for absorber with layer thickness d_1 = 15 cm, air gap thickness d_2 = 15 cm and airflow resistivity σ_1 = 1000 Pa·s/m², horizontal red lines indicate computed values of α in octave bands 125 ÷ 4000 Hz,
b) dependence of α on parameter ξ_2 for this absorber.

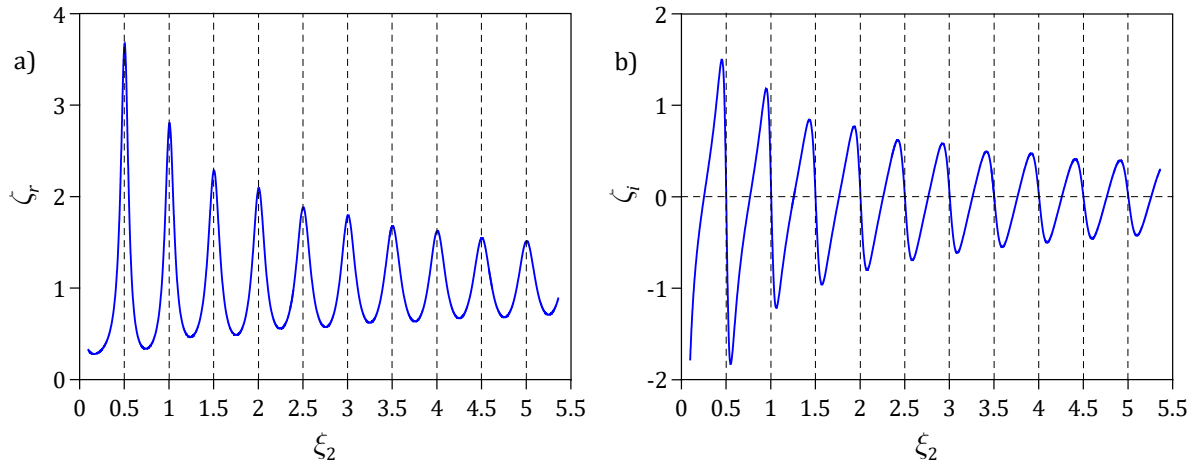

Figure 8. Changes in real (a) and imaginary (b) parts of impedance $Z_{s,1}$ with parameter ξ_2 for absorber with layer thickness d_1 = 15 cm, air gap thickness d_2 = 15 cm and airflow resistivity σ_1 = 1000 Pa·s/m².

4. Final conclusions

The work examines the absorption properties of acoustic absorbers made of fibrous materials. Calculation results obtained for a single-layer absorber backed by a hard wall have shown that the improvement of sound absorption at low frequencies can be obtained by using a material with higher airflow resistivity or by increasing the thickness of this material. On the other hand, the introduction of the air gap causes the absorption peak to shift towards lower frequencies. Unfortunately, for some frequencies a reduction of the absorption coefficient is observed due to the formation of dips with the frequency. It has been shown that peaks in the frequency relationship of the random incidence absorption coefficient are caused by a half-wavelength resonance between the front of the absorber and the hard back wall.

Acknowledgments

The authors acknowledge the financial support of the National Science Centre (NCN), Poland, under the grant agreement No. 2021/41/B/ST8/04492.

References

1. M. Meissner; Acoustics of small rectangular rooms: Analytical and numerical determination of reverberation parameters; Appl. Acoust. 2017, 120, 111–119. DOI: 10.1016/j.apacoust.2017.01.020
2. M. Meissner, T.G. Zieliński; Low-frequency prediction of steady-state room response for different configurations of designed absorbing materials on room walls; Proceedings of 29th International Conference on Noise and Vibration Engineering (ISMA 2020) and 8th International Conference on Uncertainty in Structural Dynamics (USD2020), Leuven, Belgium, September 7-9, 2020, 463–477.
3. M. Meissner; Application of high-density sound absorbing materials for improving low-frequency spectral flatness in room response; Vibrations in Physical Systems 2021, 32(1), 2021111. DOI: 10.21008/j.0860-6897.2021.1.11
4. T.G. Zieliński; Microstructure representations for sound absorbing fibrous media: 3D and 2D multiscale modelling and experiments; J. Sound Vib. 2017, 409, 112–130. DOI: 10.1016/ j.jsv.2017.07.047
5. M. Garai, F. Pompoli; A simple empirical model of polyester fibre materials for acoustical applications; Appl. Acoust. 2005, 66(12), 1383–1398. DOI: 10.1016/j.apacoust.2005.04.008
6. J. Allard, N. Atalla; Propagation of Sound in Porous Media: Modelling Sound Absorbing Materials, 2nd ed.; John Wiley & Sons, Ltd.: West Sussex, United Kingdom, 2009.
7. H. Kuttruff; Room Acoustics, 5th ed.; Spon Press: Abingdon, United Kingdom, 2009.
8. M. Delany, E. Bazley; Acoustical properties of fibrous absorbent materials; Appl. Acoust. 1970, 3(2), 105–116. DOI: 10.1016/0003-682X(70)90031-9